Symmetry between laminar and burst phases for on-off intermittency

A. Čenys
Semiconductor Physics Institute, LT-2600 Vilnius, Lithuania

A. N. Anagnostopoulos and G. L. Bleris
Physics Department, Aristotle University of Thessaloniki, GR-54006, Thessaloniki, Greece

(Received 18 February 1997)

It is demonstrated both analytically and numerically that a symmetry exists between laminar and burst phases of on-off intermittency. The symmetry is a specific feature of on-off intermittency. It does not exist for the other types of regular Pomeau-Manneville and crisis-induced intermittency. A diffusional model, which incorporates reflecting barriers representing noise and nonlinearity, predicts the same scaling for the laminar and the burst lengths near the blowout bifurcation point. The symmetry of the scaling properties is demonstrated numerically for two systems exhibiting on-off intermittency, namely, the discrete three-dimensional Hénon map and the unidirectionally coupled Rössler oscillators. [S1063-651X(97)01409-8]

PACS number(s): 05.45.+b

I. INTRODUCTION

The most interesting feature of the intermittency in dynamic systems is its universality. The few universality classes with the corresponding scaling exponents describe very well the statistical properties of the intermittency in a large variety of models as well as in experimental systems. The universal scaling is related to the universal dynamics of the various systems in the neighborhood of an invariant object responsible for the intermittency. In the case of Pomeau-Manneville intermittency [1] such invariant objects in the phase space are fixed points or periodic orbits. The laminar phases correspond to the time periods when the trajectory stays in the neighborhood of the invariant object. Dynamics in this region can be described by linear equations. Linear dynamics, however, does not ensure reinjection to the neighborhood of the invariant object and the trajectory always leaves the linear neighborhood of the unstable fixed point or periodic orbit during the burst phase. As a result, properties of the burst phases are not universal since the nonlinear dynamics far from the invariant object is system dependent.

Recently, a different type of intermittency [2], named by Platt *et al.* [3] on-off intermittency, has attracted wide attention. It is extensively studied both analytically and numerically [4–6] and is observed in various experimental systems [7,8]. On-off intermittency can be defined as an intermediate case between Pomeau-Manneville [1] and crisis-induced intermittency [9]. It possesses for the laminar lengths the same scaling exponents as that of Pomeau-Manneville type-III intermittency. Time series of the generic variable, however, look like that of the chaos-to-chaos intermittency [8]. The distinguishing feature of the on-off intermittency is a particular structure of the phase space. It possesses a smooth invariant manifold containing a chaotic attractor. This structure of the phase space is typical for dynamical systems with symmetry, for example, coupled, identical chaotic systems. The smooth invariant manifold can be obtained from the symmetry properties of the equations describing the dynamics of the system. It can be quite difficult, however, to detect the invariant manifold from the time series.

In this paper we demonstrate a different symmetry feature of the on-off intermittency, which can be easily observed in experimental time series and is typical only for this type of intermittency. The symmetry between laminar and burst phases can be easily detected visually. A signal, typical for on-off intermittency, is presented in Fig. 1 both as a time series of the variable r_n corresponding to the distance from the invariant manifold and as a time series of the inverse variable r_n^{-1}. The similar structures of both time series are evident. It will be shown below that both time series not only

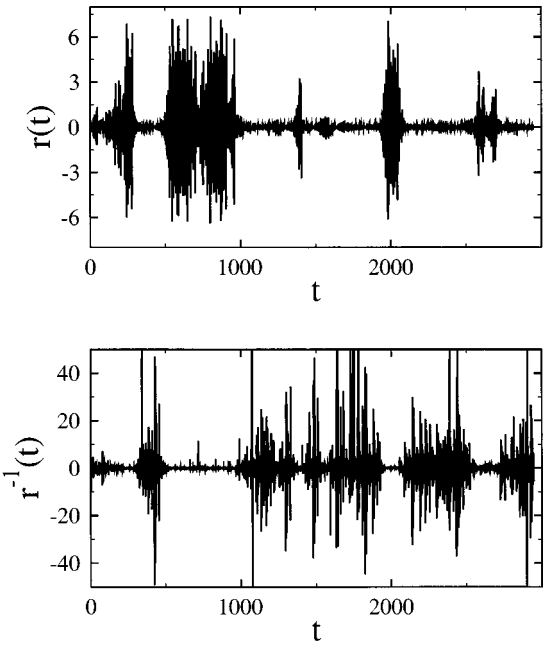

FIG. 1. Intermittent time series calculated numerically for the unidirectionally coupled noisy Rössler oscillators just above the blowout bifurcation point. Details of the model are given in Sec. III. r_n defines the difference between the y variables of both identical oscillators. The inverse variable r_n^{-1} is plotted taking into account only local minimum and maximum points in the original time series and corresponds to the inverse envelope.

look similar but also have the same scaling properties. To obtain reasonable time series of the inverse signal for continuous time systems like that of coupled Rössler oscillators in Fig. 1, the envelope including only local minima and maxima points should be plotted.

The on-off intermittent bursting takes place only above the blowout bifurcation point [10] at which the largest transversal Lyapunov exponent becomes positive for noise-free, perfectly symmetric, dynamical systems. Below the blowout bifurcation there are no bursts since the trajectories attracted to the invariant manifold stay on it forever. In noisy and/or slightly asymmetric systems bursts occur also below the noise-free bifurcation point. In this more realistic case, the symmetry between laminar and burst phases is even more extended. The noisy on-off intermittency can be presented as a switching between two limiting states completely controlled by noise and by nonlinearity correspondingly. Both limiting states are unstable and switching between them takes place, causing the intermittent temporal behavior. The reason for the symmetry between laminar and burst phases is that both noise and nonlinearity do not influence essentially the dynamics in the region between the two limiting states. They only ensure that the system is bounded, i.e., that the trajectories cannot be attracted forever both by the invariant manifold and by some other attractor in the phase space far from the manifold. The dynamics in the region between two limiting states is determined by the symmetric random or ''chaotic'' walk.

II. DIFFUSIONAL MODEL

The statistical properties of the burst phases, like that of the laminar phases, can be obtained from the analysis of the simple one-dimensional map

$$r_{n+1}=ax_n r_n, \tag{1}$$

where a is a control parameter. It describes the dynamics of the distance r_n from the invariant manifold located at $r_n=0$. The chaotic driving variable x_n is determined by the dynamics on the manifold. This map has been studied extensively in order to obtain analytical scaling properties of the laminar phases. We exploit the same approach as that used to calculate the mean laminar length [5] and the distribution of the laminar lengths [6] for noisy on-off intermittency. The influence of additive noise is modeled by a reflecting boundary at some level r_1, representing the noise strength in these studies. The barrier reflects the most important consequence of the additive noise, i.e., fast repulsion from the close neighborhood of the invariant manifold. In a similar way, the influence of nonlinear terms can be taken into account by incorporating a second reflecting barrier at $r_2 \geqslant r_1$. The second barrier reflects the fact that there is no other attractor in the phase space far from the invariant manifold and the system cannot runaway.

The map (1) in the logarithmic domain corresponds to the biased ''chaotic'' walk

$$\ln|r_{n+1}|=\ln|r_n|+v+\beta_n \tag{2}$$

bounded by the two reflecting boundaries $\ln r_1$ and $\ln r_2$. The new control parameter $v=(a-a_c)/a_c$ defines a deviation from the blowout bifurcation point $|a_c|=\exp(-\langle\ln|x_n|\rangle)$. Here angular brackets denote the time average. The new driving variable $\beta_n=\ln|x_n|-\langle\ln|x_n|\rangle$ has zero mean value $\langle\beta_n\rangle=0$. The dispersion D of the variable β_n is related to the dispersion of the local Lyapunov exponents of the original chaotic driving signal [5]. Most of the analytical results for the laminar lengths are obtained assuming the driving chaotic variable β_n to be uncorrelated Gaussian noise. This assumption essentially simplifies the analysis and provides good results for the long-time behavior close to the noise-free blowout bifurcation point. The random walk is symmetric at the bifurcation point $v=0$ and all results obtained for the laminar lengths should also hold for the burst lengths, provided the noise barrier r_1 is replaced by the nonlinearity barrier r_2. The control parameter v should be replaced by $-v$ to obtain the results for the burst phases in the case of small deviations from the bifurcation point.

The diffusional model predicts the same universal distribution

$$P(\tau)\propto\sum_{i=0}^{\infty}(2i+1)^2\exp\left[-(2i+1)^2\frac{\tau}{\tau_0}\right] \tag{3}$$

for both laminar and burst phases at the bifurcation point $v=0$. It is obtained from the analysis of the corresponding Fokker-Planck equation [6]. The characteristic time of the exponential decay is given by

$$\tau_0=\frac{8\ln^2 r^*}{\pi^2 D}. \tag{4}$$

It depends on the noise level r_1 for the distribution of the laminar lengths ($r^*=r_{th}/r_1$). For the distribution of the burst lengths it depends on the barrier r_2 characterizing nonlinear terms ($r^*=r_2/r_{th}$). In both cases, however, it obeys the same logarithmic dependence on the threshold value r_{th}.

For medium and large lengths τ, the universal distribution (3) is well approximated by a power law and an exponential asymptotic, respectively

$$P(\tau)\propto\begin{cases}\tau^{-3/2}, & \tau\leqslant\tau_0\\ \exp\left[-\dfrac{\tau}{\tau_0}\right], & \tau\geqslant\tau_0.\end{cases} \tag{5}$$

The exponential asymptotic behavior describes both the fast exponential falloff and the shoulder region above the power-law straight line. This shoulder appears because of the absence of the multiplier $\tau^{-3/2}$ in the asymptote (5) for the large lengths. It is clearly seen in the numerically obtained distributions presented below. There are only two regions corresponding to the different behaviors of the universal distribution with a narrow crossover region between them [6].

A similar analysis based on the Fokker-Planck equation gives the expression valid both for mean laminar and for mean burst lengths [5],

$$\langle\tau\rangle = z^* v^{*-1} + 2Dv^{-2}\exp(-2v^* D^{-1}\ln r^*) \times[1-\exp(2v^* z^* D^{-1})]. \quad (6)$$

Here, for laminar lengths $v^* = v$ and for burst lengths $v^* = -v$. The parameter z^* defines the reinjection to the region below and above the threshold r_{th} for laminar and burst phases, repectively. It satisfies the condition $|v|z^* D^{-1} \ll 1$ for diffusional reinjection. The dependence of the parameter z^* on the threshold r_{th}, discriminating the laminar and the burst phases, is weak [5].

The noise-free scaling $\langle\tau\rangle \propto v^{-1}$ of the mean laminar lengths appears only in the region $vD^{-1}\ln(r_{th}/r_1) \gg 1$ above the critical point for the noisy on-off intermittency. The similar scaling for the mean burst length $\langle\tau\rangle \propto -v^{-1}$ appears below the critical point in the region $|v|D^{-1}\ln(r_2/r_{th}) \gg 1$. It is rather difficult, however, to observe this scaling in real systems since the nonlinear terms, not included in the diffusional model, begin to play an important role moving away from the bifurcation point. As a result, the above scaling occurs only in a limited region that is difficult to detect. The dependence of the mean length on the threshold at the critical point $v = 0$ given by

$$\langle\tau\rangle = \begin{cases} 2D^{-1} z^* \ln(r_{th}/r_1) & \text{for laminar lengths} \\ 2D^{-1} z^* \ln(r_2/r_{th}) & \text{for burst lengths} \end{cases} \quad (7)$$

is a characteristic more convenient for the detection of the symmetry between laminar and burst phases from time series data. A single record of the intermittent time series at the critical point is sufficient to observe the logarithmic dependence of the mean length $\langle\tau\rangle$ on threshold r_{th}.

III. NUMERICAL RESULTS

The diffusional model described above does not take into account all details of the chaotic systems. We present below numerical results obtained from two models that demonstrate that the symmetry between laminar and burst lengths holds also for real systems exhibiting on-off intermittency. The first model is a discrete time system, namely, the three-dimensional (3D) Hénon map [8,11]

$$x_{n+1} = F(x_n, x_{n-1}) + a[x_n^2 - F^2(x_{n-1}, x_{n-2})] + k\eta_n,$$
$$F(x_n, x_{n-1}) \equiv 1 + 0.3x_{n-1} - 1.4x_n^2, \quad (8)$$

where k defines the small amplitude of the additive random noise η. The invariant manifold $r_n \equiv x_n - F(x_{n-1}, x_{n-2}) = 0$ in the phase space of the map (8) exists for any value of the control parameter a in the noise-free case $k = 0$. The manifold is stable below the blowout bifurcation point $a_c = 0.933\ldots$ and contains a chaotic attractor corresponding to the well-known Hénon attractor. The noise-free model exhibits on-off intermittency above the bifurcation point $a > a_c$ at which the invariant manifold becomes unstable. The map (8) was introduced in [11] as a particular example from the class of maps generating identical attractors.

In recent years coupled, identical, chaotic systems have attracted wide attention due to their very interesting feature of chaotic synchronization and their possible applications in secure communications. The on-off intermittency is a common phenomenon appearing near the threshold of synchronization for most of the coupled, identical, chaotic systems. For noisy or slightly nonidentical systems, the intermittent bursting takes place below as well as above the noise-free blowout bifurcation point, essentially affecting the synchronization required in the applications. As a second continuous-time model we have studied numerically the unidirectionally coupled Rössler oscillators

$$dx/dt = -y - z,$$
$$dy/dt = x + 0.2y + a(y_1 - y) + k\eta, \quad (9)$$
$$dz/dt = 0.2 + z(x - 5.7),$$

where the driving variable y_1 is generated by the another identical Rössler oscillator.

The distribution of the laminar and burst lengths is the most convenient characteristic for the estimation from numerical as well as experimental time series data. Recording a single but long enough time series at the bifurcation point is sufficient to estimate the distribution. Moreover, the fine tuning of the control parameter is not necessary since the power-law scaling both for laminar and for burst lengths appears in

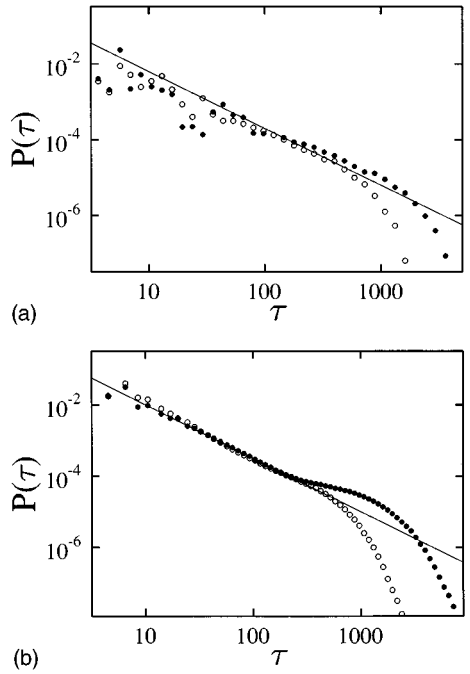

FIG. 2. (a) Distribution of the laminar lengths (filled circles) and the burst lengths (open circles) for coupled Rössler oscillators at the bifurcation point $a_c = 0.123$ as estimated from the zero transversal Lyapunov exponent. The threshold r_{th} is 0.5 for laminar lengths. For burst lengths $r_{th} = 0.1$. An additive random noise with amplitude 0.01 is added at every integration step $h = 0.01$ in a fourth-order Runge-Kutta algorithm. (b) Same as (a) but for the 3D Hénon map with very small noise ($k = 10^{-6}$) at the bifurcation point $a_c = 0.933$. $r_{th} = 5 \times 10^{-3}$ for laminar lengths and $r_{th} = 5 \times 10^{-5}$ for burst lengths. For both systems the probability is estimated using equispaced in the logarithmic scale, properly weighted boxes in order to have uniformly distributed values. The solid straight line corresponds to the power law with the exponent $-3/2$.

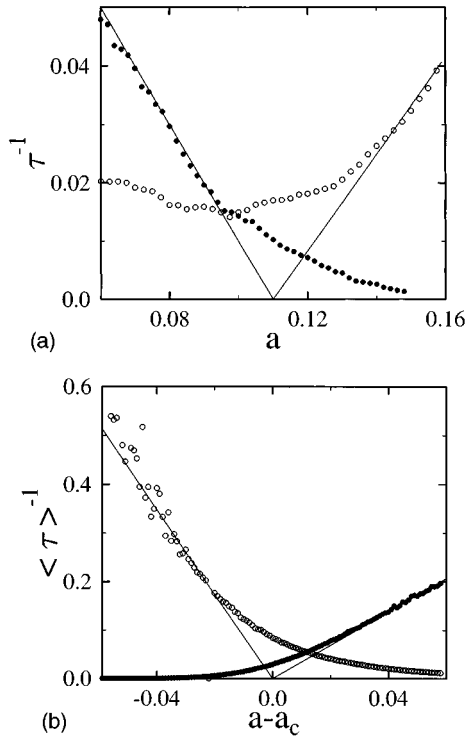

FIG. 3. (a) Dependence of inverse mean laminar lengths (filled circles) and mean burst lengths (open circles) on the control parameter a for coupled, slightly nonidentical Rössler oscillators without noise (the parameter in the third equation is changed to 5.75 for the driving Rössler oscillator). The threshold $r_{th}=0.5$ is the same for both laminar phases and burst phases. (b) Same as (a) but for the noisy 3D Hénon map ($r_{th}=5\times10^{-4}$). The straight lines are drawn only to guide the eye.

the region above as well as below the bifurcation point for the noisy and/or for the slightly asymmetric case typical in the experimental situation. For noise-free and completely symmetric systems the power law in the distribution can be observed also slightly above the bifurcation point. Numerically calculated distributions of both laminar and burst lengths for the 3D Hénon map and for the coupled Rössler oscillators are shown in Figs. 2(a) and 2(b), respectively. All distributions have a pronounced power-law scaling in the range of medium lengths τ. The shoulder above the power-law straight line, preceding the fast exponential falloff, is better pronounced in the distribution of laminar lengths. The reason is that the shoulder appears due to the so-called diffusional echo from the reflecting boundaries and it disappears if the reflecting boundary is not ''hard'' enough. The diffusional model assumes that both noise and nonlinearity barriers are identical and predicts that the distributions of the laminar and the burst lengths are identical. In the real systems, however, the nonlinearity barrier responsible for the shoulder in the distribution of the burst lengths is quite ''soft.'' The influence of the nonlinear terms becomes important in the region in which the trajectory, visiting it once, can stay for a long time. The noise-induced barrier is much ''harder'' since noise rejects the trajectory very fast from the too close neighborhood of the invariant manifold.

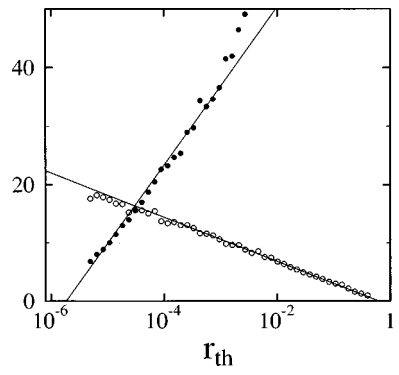

FIG. 4. Dependence of inverse mean laminar length (dots) and burst lengths (circles) on the threshold r_{th} for the noisy 3D Hénon map at the bifurcation point. Solid lines correspond to the scaling predicted by the diffusional model.

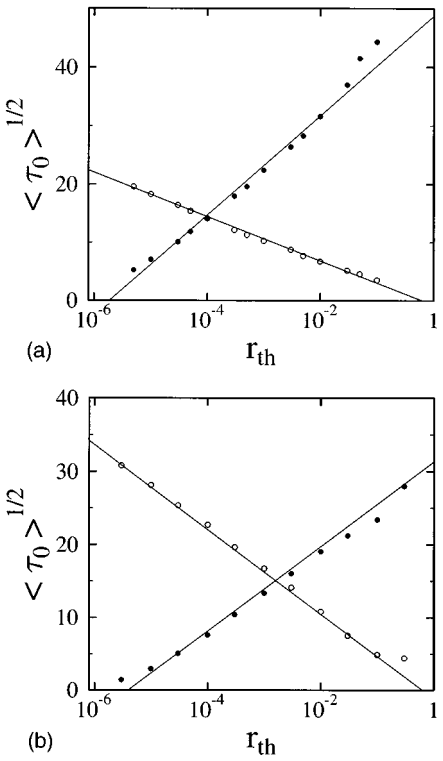

FIG. 5. Parameter τ_0 of the exponential falloff in the distributions of the laminar length (dots) and burst lengths (circles) versus the threshold r_{th} for (a) the noisy 3D Hénon map and (b) the artificial linear system with reflecting barriers modeling the additive noise and the nonlinearity and driven by the Hénon map. Solid lines correspond to the scaling predicted by the diffusional model.

Another universal scaling law often observed is the linear dependence of the inverse mean laminar length on the deviation from the bifurcation point. In its pure form it appears above the blowout bifurcation point for noise-free on-off intermittency. The identical scaling behavior is expected for burst lengths below the bifurcation point in the model with noise but without nonlinearity. However, even numerical models without nonlinear terms are very artificial. For real systems linear scaling of the inverse mean laminar and burst lengths can be observed only in the limited range of the control parameter above and below the bifurcation point, respectively. The possibility to detect this region is very sensitive to the noise level. The situation becomes even more complicated for noise-free but slightly nonidentical coupled

systems. In this case, the blowout bifurcation point itself cannot be estimated precisely since two slightly different manifolds corresponding to each of the coupled systems exist. The problem concerning the reliable estimation of the scaling region is seen in Fig. 3, though a symmetry between mean laminar and mean burst lengths is evident.

The identical scaling of laminar and burst lengths is better pronounced in characteristics estimated at the noise-free bifurcation point. The distribution of τ is only one example of such characteristics. For the noisy 3D Hénon map we have calculated numerically also the dependence of the mean length $\langle \tau \rangle$ and of the parameter τ_0 on the threshold r_{th} as shown in Figs. 4 and 5, respectively. τ_0 defines the fast exponential falloff for large lengths τ in the distributions $P(\tau)$. These characteristics are conveniently estimated from the time series data since calculations for the different threshold values discriminating laminar and burst phases can be performed just from a single time series. As it can be deduced from Figs. 4 and 5 the logarithmic dependence predicted by the diffusional model holds for a wide range of threshold values for both laminar and burst lengths. However, the agreement between the diffusional model and the numerical results is not complete. The model predicts not only the same scaling but also the same absolute values of the proportionality factor. The corresponding slopes in Figs. 4 and 5(a) are clearly different for laminar phases and bursts. Although predicting the correct scaling, the diffusional model incorporating reflecting barriers is not sufficient to describe all quantitative details of the on-off intermittency. To prove that different slopes are emanating from the not completely adequate description of the noise and nonlinearities by the reflecting barriers, we have calculated the same dependence of τ_0 on r_{th} for the artificial model. The model corresponds to the noise-free linear chaotic walk with the driving signal generated by the Hénon map like in the case of the 3D one. The reflecting barriers were explicitly incorporated in numerical simulations. As it can be seen in Fig. 5(b), for this model not only the scaling but also the slopes are the same for both the laminar and the burst phases.

IV. CONCLUSION

We have shown that a symmetry between laminar and burst phases for the on-off intermittency exists. It can be detected visually if the intermittent time series is compared with that of the inverse variable. The diffusional model of on-off intermittency introduced earlier predicts a complete symmetry between laminar and burst phases. It incorporates reflecting barriers to model the influence of random additive noise and nonlinearities. A numerical analysis of the noisy 3D Hénon map and the unidirectionally coupled Rössler oscillators shows that for real systems exhibiting on-off intermittency only the scaling laws appear to be symmetric, but not the proportionality factors. This result is explained by the fact that reflecting boundaries represent only a rough approximation for additive random noise and nonlinear terms.

ACKNOWLEDGMENT

This work was partially supported by the EEC under Contract No. CIPA-CT93-0255.

[1] Y. Pomeau and P. Manneville, Commun. Math. Phys. **74**, 189 (1980).

[2] A. S. Pikovsky, Z. Phys. B **55**, 149 (1984); H. Fujisaka and H. Yamada, Prog. Theor. Phys. **74**, 918 (1985); **75**, 1087 (1986); L. Yu, E. Ott, and Q. Chen, Phys. Rev. Lett. **65**, 2935 (1990); T. Kapitaniak, Prog. Theor. Phys. **92**, 1033 (1994).

[3] N. Platt, E. A. Spiegel, and C. Tresser, Phys. Rev. Lett. **70**, 279 (1993).

[4] A. S. Pikovsky and P. Grassberger, J. Phys. A **24**, 4587 (1991); J. F. Heagy, N. Platt, and S. M. Hammel, Phys. Rev. E **49**, 1140 (1994); P. Ashwin, J. Buescu, and I. Stewart, Phys. Lett. A **193**, 126 (1994); E. Ott, J. C. Alexander, I. Kan, J. C. Sommerer, and J. A. Yorke, Physica D **76**, 384 (1994); S. C. Venkataramani, T. M. Antonsen, Jr., E. Ott, and J. C. Sommerer, Phys. Lett. A **207**, 173 (1995); M. Ding and W. Yang, Phys. Rev. E **52**, 207 (1995); Y. Lai, *ibid.* **54**, 321 (1996); S. C. Venkataramani, B. R. Hunt, and E. Ott, *ibid.* **54**, 1346 (1996).

[5] A. Čenys and H. Lustfeld, J. Phys. A **29**, 11 (1996).

[6] A. Čenys, A. Anagnostopoulos, and G. Bleris, Phys. Lett. A **224**, 346 (1997).

[7] P. W. Hammer, N. Platt, S. M. Hammel, J. F. Heagy, and B. D. Lee, Phys. Rev. Lett. **73**, 1095 (1994); Y. H. Yu, K. Kwak, and T. K. Lim, Phys. Lett. A **198**, 34 (1995); A. Čenys, A. Namajūnas, A. Tamaševičius, and T. Schneider, *ibid.* **213**, 259 (1996).

[8] F. Rodelsperger, A. Čenys, and H. Benner, Phys. Rev. Lett. **75**, 2594 (1995).

[9] C. Grebogi, E. Ott, and J. A. Yorke, Phys. Rev. Lett. **48**, 1507 (1982); C. Grebogi, E. Ott, F. J. Romeiras, and J. A. Yorke, Phys. Rev. A **36**, 5365 (1987).

[10] E. Ott and J. C. Sommerer, Phys. Lett. A **188**, 39 (1994).

[11] A. Čenys, Europhys. Lett. **21**, 407 (1993).